Instrumentation and Technique for Deducing Cloud Optical Depth

R. A. RASCHKE AND S. K. COX

Department of Atmospheric Science, Colorado State University, Fort Collins, CO 80523

(Manuscript received 10 January 1983, in final form 10 July 1983)

ABSTRACT

The feasibility of using a photodiode radiometer to infer optical depth of thin clouds from solar intensity measurements is examined. Data were collected by a photodiode radiometer which measured incident radiation at angular fields of view of 2, 5, 10, 20 and 28°. Values of normalized annular radiance and transmittance were calculated from the observations and compared to similar calculations from a Monte Carlo radiative transfer model. The Monte Carlo results were for cloud optical depths of 1 through 6 over a spectral bandpass of 0.3 to 2.8 μm.

Eight case studies including high, middle and low clouds were examined. Experimental values of cloud optical depth were determined by comparing plots of transmittance versus field of view with the model calculated curves and from the average of the five optical depths calculated for each field of view. Analysis of the case study results indicates that the photodiode radiometer can be used effectively to determine the optical depth of thin clouds.

1. Introduction

The potential impact of clouds on the earth's radiation budget and subsequently upon the climate has been acknowledged for over a century. However, a clear understanding of the magnitude of the effect and even whether clouds represent a positive or a negative feedback upon climate still eludes us. A significant portion of this lack of understanding comes from a lack of knowledge of the variability of the radiative properties of clouds. The magnitude and the sign of the effect of clouds upon terrestrial climate depends upon not only cloud cover and cloud height, but also upon the average solar reflectance and transmittance of the clouds and the clouds' infrared emittance. This effect is clearly shown in the work of Manabe and Strickler (1964), Cox (1971) and Bowling (1972).

Several authors have discussed the possible effects of clouds on climate. Cess (1976) and Cess and Ramanathan (1978) suggest that cloud amount is not important in establishing global climate because the effects of changes in infrared opacity are exactly compensated by the effects caused by changes in cloud albedo. On the contrary, Ellis (1978) and Ohring and Clapp (1980) found that clouds are significant feedback mechanisms with the albedo effect dominating the greenhouse effect. One way to proceed in seeking a better understanding of the role of clouds in the global climate system is to collect data representing the radiative and physical properties of clouds and then repeating analysis of the types referred to earlier. One such convenient radiative parameter is cloud optical depth. Ohring and Adler (1978) used a zonally averaged climate model in which a single cloud layer was assumed at each latitude belt. A specified cloud amount, altitude, and optical depth were given for the cloud layer. Since the albedo of the cloud depends on the cloud optical depth, the concept of optical depth is very important in this model. Ohring and Adler assigned optical depths of 2, 8, and 16 to high, middle, and low clouds respectively. It would be beneficial, then, to be able to make actual measurements of cloud optical depths and apply them in the various climate models.

The primary objective of this paper is to determine the feasibility of using a photodiode radiometer to deduce the optical depth of thin clouds. Our method is an extension of the work reported by Thompson and Cox (1982) who used data from a normal incidence pyrheliometer to measure the changing transmittance of the direct solar beam. In the present work a relationship is established between the bulk scattering properties of a cloud and its optical depth; actual measurements of the angular dispersion of energy from the direct beam in the presence of clouds are compared with results from computations made with a Monte Carlo radiative transfer model. An instrument consisting of five silicon photodiode detectors, each with a different angular field of view, was used to measure the energy scattered at small angles from the direct beam. These data were compared with the results obtained from a Monte Carlo radiative transfer model.

Coulson (1975) presents the classical definition for the optical depth above a height z as

$$\tau(\lambda, z) = \int_z^{z_i} B(\lambda, z)dz, \tag{1}$$

where B is the attenuation coefficient. The value of $\tau(\lambda, z)$ is related by an exponential relationship to the spectral transmittance of the medium from z to z_i where z is some height within the atmosphere and z_i is the top of the atmosphere. In this study we shall seek an empirical relationship between a spectrally averaged value of the cloud optical depth and a set of observations easily made from the ground.

The feasibility of using photodiode radiometer measurements to deduce cloud optical depth was examined using data collected for various cloud types. These observations were compared with computations made using the Monte Carlo radiative transfer model (McKee and Cox, 1974; Davis *et al.*, 1979) with a Best (1951) cloud droplet distribution. Model results were generated for broadband (0.3–2.8 μm) cloud optical depths of 1 to 6. A graphical comparison was made using plots of measured transmittance versus field of view. Regression equations were also derived between optical depth and the broadband transmittance values.

The study was limited to optically thin clouds ($\tau < 6$) because the largest variability in observed transmittance occurs in the range of optical depths from 0 to 10. In addition, the value of transmittance becomes very small for larger values of τ (Thompson and Cox, 1982). A plot of modeled transmittance versus optical depth in Fig. 1 confirms the fact that the greatest variability in the transmittance occurs at optical depths less than 6.

2. Instrumentation

a. Description

Data were collected from three instruments mounted on an equatorial tracking system and located at the Atmospheric Science facility at Colorado State University. An Eppley pyrheliometer was used to measure the direct component of the incident solar radiation. An Eppley pyranometer was used to measure the total radiation in a plane perpendicular to the direct solar beam. The third radiometer, especially designed for this study, is really five instruments in one. This device employed five silicon photodiodes each collimated to achieve a different full angle field of view. Table 1 lists the fields of view of the five photodiodes and the dimensions of the collimator tubes used to achieve these fields of view. A schematic diagram of the instrument is shown in Fig. 2.

TABLE 1. Dimensions of the collimator tubes.

Field of view (deg)	Length (mm)	Aperture size (mm)
1.99	144.8	2.5
5.05	57.2	2.5
9.87	29.2	2.5
20.54	14.0	2.5
28.04	10.2	2.5

The silicon photodiodes used were series PV-100A manufactured by EG&G Electro-Optics Division.

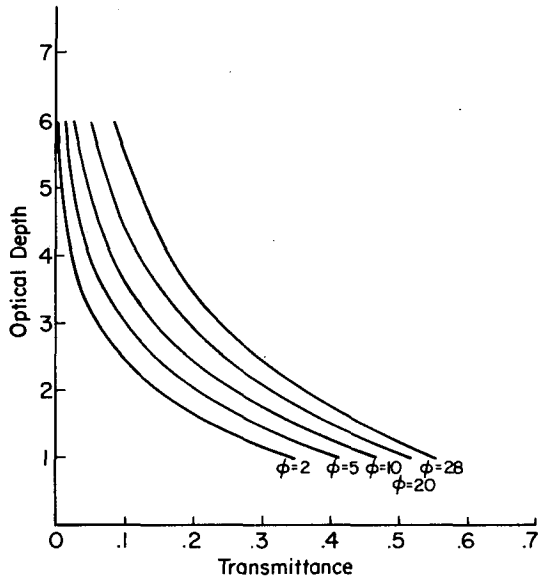

FIG. 1. Optical depth versus transmittance for fields of view ϕ = 2, 5, 10, 20 and 28° produced from the Monte Carlo model.

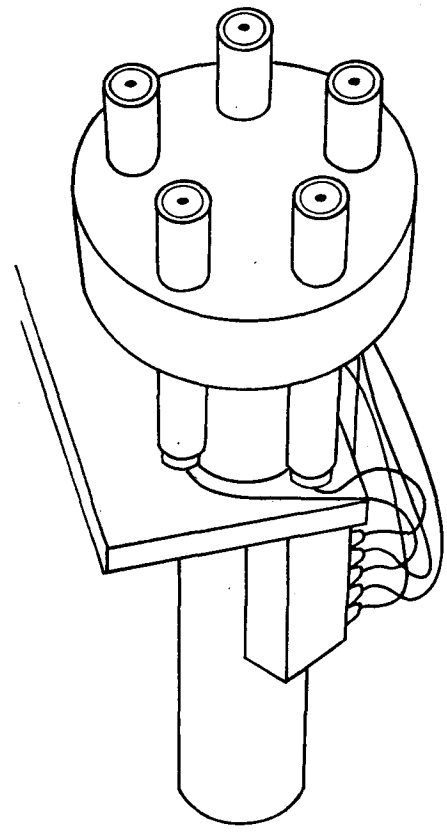

FIG. 2. Schematic diagram of multiple field of view photodiode radiometer.

These photodiodes have a spectral bandpass from 0.35 μm to 1.15 μm.

The photodiodes produce a current signal which is directly proportional to the amount of incident radiation striking the active area. This current signal was converted to a voltage signal through the use of a current to voltage amplifier.

The collimators, whose dimensions were given in Table 1, consisted of cylindrical tubes with circular aperatures at the top, bottom and midway along the length. All interior surfaces of the collimator were painted with an optically flat black paint.

b. Calibration

A cloud-free day was chosen to perform a relative calibration for the photodiodes. The 2° field of view (FOV) instrument was chosen as a relative standard and the other four photodiodes were compared with it. The photodiode outputs were recorded for a clear case and for a case where a diffusing plate was present. In this way, photodiode sensitivities could be determined when both large and small signals were present. The photodiode sensitivities were determined by dividing the 2° photodiode voltage by the voltages from the other four photodiodes for the diffuse and clear sky cases. The final sensitivity of the photodiodes was taken to be the average of the diffuse case sensitivity and the clear case sensitivity.

The photodiode relative sensitivities were then related to broadband shortwave radiation using a linear relationship between the 5° FOV silicon detector and the Eppley pyrheliometer which also has a 5° FOV.

3. Radiative transfer model

Actual photodiode radiometer measurements of the angular dispersion of energy from the direct beam in the presence of clouds were compared with results from theoretical computations made with a semi-infinite Monte Carlo model. The Monte Carlo model is a multiple scattering model described by McKee and Cox (1974) and Davis *et al.* (1979).

The Monte Carlo model was run for spectral bandpass of 0.3 to 0.8 and 0.8 to 2.8 μm. The combined 0.3 to 2.8 μm spectral interval was chosen because it corresponds to the spectral response of the pyrheliometer and pyranometer.

The model output includes the number of photons that exit the base of the cloud at various scattering angles from the incident beam. Photons are counted for annular rings with widths of 0–2, 2–5, 5–10, 10–20, 20–28 and 28–180°. The model also determines the energy that reaches the ground in each annular ring, the energy absorbed by both the atmosphere and the cloud, and the energy leaving the top of the atmosphere. Model calculations were made assuming a Best (1951) droplet distribution for water clouds. The total amount of transmitted, reflected and absorbed energy in the 0.3–2.8 μm spectral bandpass was determined by adding the values obtained in the 0.3–0.8 and 0.8–2.8 μm regions. Modeled transmittance values, which correspond to the photodiode measurement divided by the incident radiation at the top of the atmosphere, were calculated from the model results for each full angle field of view, i.e., 0–2, 0–5, 0–10°, etc., by dividing the energy incident at the surface in a particular field of view by the solar constant. Table 2 lists the transmittance values calculated from the model results for each cloud optical depth for the case of a zero degree zenith angle.

4. Data reduction procedures

The voltage of the 5° field of view photodiode was forced to correspond to the irradiance value of the pyrheliometer, which has a field of view of very near 5°. The irradiance values for the 2, 10, 20 and 28° field of view photodiodes were then adjusted by using relative sensitivities (derived previously), which relate the output of these detectors to the 5° detector. Transmittance values for each field of view were determined by dividing the irradiances by the solar constant corrected for sun-earth distance for the 0.3–2.8 μm region. These transmittances could then be compared to those found from the Monte Carlo model.

5. Comparison of model and experimental results

a. Procedures

Two methods are used to compare actual measurements made with the multiple photodiodes to the results obtained from the Monte Carlo radiative transfer model. First, model values of transmittance versus field of view are compared graphically with experimental values for cloud optical depths of 1 to 6. Instantaneous values and 10 min average values of transmittance obtained from the photodiode measurements were plotted and compared to the model values.

A second method used to calculate optical depth is to plot the optical depth versus modeled transmittance for each field of view. A plot of this form is shown in

TABLE 2. Transmittance values calculated for cloud optical depths of 1 to 6.

Angular aperature (deg)	Optical depth τ					
	1	2	3	4	5	6
0–2	0.3461	0.1414	0.0604	0.0253	0.0104	0.0049
0–5	0.4131	0.1997	0.1017	0.0501	0.0251	0.0141
0–10	0.4667	0.2543	0.1437	0.0804	0.0467	0.0282
0–20	0.5176	0.3162	0.2003	0.1275	0.0832	0.0592
0–28	0.5521	0.3584	0.2423	0.1652	0.1181	0.0870
0–180	0.8080	0.7568	0.7056	0.6616	0.6188	0.5770

Fig. 1. To relate transmittance to optical depth, an equation is then found for each of the curves in Fig. 1. The equations of the curves yield a value of optical depth for each of the five fields of view when the transmittance values for each FOV are inserted. The optical depth of the cloud is then taken to be the average value of the five optical depths predicted by the equations. The equations of the curves of Fig. 1 have the form:

$$\tau = a + b \ln T. \quad (2)$$

The a and b coefficients of Eq. (2) are listed in Table 3. Although the relationship expressed in Eq. (2) contains no explicit dependence on solar zenith angle, in reality, a zenith angle dependence does exist. In order to minimize this dependence we define a slant-path optical depth of the cloud, which is the optical depth of the cloud multiplied by the secant of the solar zenith angle. Table 4 lists calculated transmittance values for selected, paired cases that contain equal slant-path optical depths for different zenith angle combinations. It is clear from this comparison that the major impact of the zenith angle dependence is accounted for by the slant-path optical depth concept for zenith angles less than 60° and optical depths less than 6. Both instantaneous and 10 min average values of transmittance were used to calculate the cloud optical depths.

Before inspecting the results, let us define an evaluation procedure to determine how well the measured optical depths agree with the graphical predictions. From the equations of the curves in Fig. 1, values of transmittance that would be produced by the Monte Carlo model can be calculated for optical depths close to the experimental value. To determine if the calculated values are really representative of the data points, the optical depth producing the smallest rms error between the calculated and experimental transmittances may be found. The smallest rms error indicates the model curve that best fits the experimental values.

b. Results

In this section we shall examine representative data collected for various cloud types. Fig. 3 shows the plots of transmittance versus field of view for both 1 and 10 min time periods for the cloud situations examined.

TABLE 3. Coefficients of the curves relating modeled transmittance to optical depth for the five fields of view. The equations have the form $\tau = a + b \ln T$.

FOV	a	b	Correlation coefficient
2°	−0.26906	−1.1666	0.99948
5°	−0.34655	−1.4681	0.99901
10°	−0.41304	−1.7754	0.99911
20°	−0.58852	−2.2697	0.99763
28°	−0.72527	−2.6923	0.99634

TABLE 4. Comparison of transmittance values for paired cases with the same slant-path optical depth.

$\tau_{\theta=0°}$	θ	$T_{0\text{-}2°}$	$T_{0\text{-}5}$	$T_{0\text{-}10}$	$T_{0\text{-}20}$	$T_{0\text{-}30}$
1	30°	0.3200	0.3218	0.3258	0.3430	0.3661
1.15	0°	0.3137	0.3151	0.3190	0.3339	0.3547
1	60°	0.1376	0.1390	0.1429	0.1589	0.1809
2	0°	0.1358	0.1374	0.1417	0.1594	0.1840
2	30°	0.1031	0.1046	0.1099	0.1284	0.1537
2.29	0°	0.0988	0.1006	0.1053	0.1241	0.1485
2	60°	0.0202	0.0210	0.0238	0.0357	0.0493
4	0°	0.0209	0.0224	0.0274	0.0482	0.0714
4	30°	0.0097	0.0109	0.0143	0.0296	0.0477
4.59	0°	0.0180	0.0134	0.0182	0.0364	0.0590
4	60°	0.0003	0.0005	0.0017	0.0068	0.0136
8	0°	0.0004	0.0015	0.0048	0.0176	0.0350

The crosses represent the observed data and the dashed lines represent the transmittance versus FOV relationships for an optical depth equal to the average deduced from the five different FOV sensors.

The measured points compare favorably with what is predicted from theory, especially for the instantaneous cases presented; however, there are several exceptions. The 10 min average values of transmittance for both the 26 and 28 October cases are significantly different from what would be expected from the model results. The 26 October case is particularly interesting. The three small fields of view predict a lower optical depth than the two wider fields of view. The same situation appears on 15 April but to a much greater degree. The last two periods are mentioned because the spatial nonuniformity of the clouds is believed to be responsible for the seemingly inconsistent results. On 26 October, an area around the sun was covered by cirrocumulus clouds of moderate optical thickness; however, a very dense altocumulus deck was located near the sun's position. This altocumulus layer was most likely responsible for reducing the energy reaching the wide field of view detectors.

On 15 April, a broken cumulus field was present. The measured points in the figures show the effect of the sun being in an optically thin region of the cloud surrounded by much denser clouds.

The feature where the small fields of view suggest smaller optical depths than those of the wide fields of view sensors is present in many of the figures. As mentioned above, the type of cloud cover appears to be responsible for magnifying or producing this effect in some cases. The fact that this feature appears to some degree in all but the 28 October case suggests that something other than cloud cover may be at least partially responsible. A possible explanation is the fact that the model curves were produced using a cloud with a Best distribution for spherical water droplets. In most of the cases examined only ice clouds were

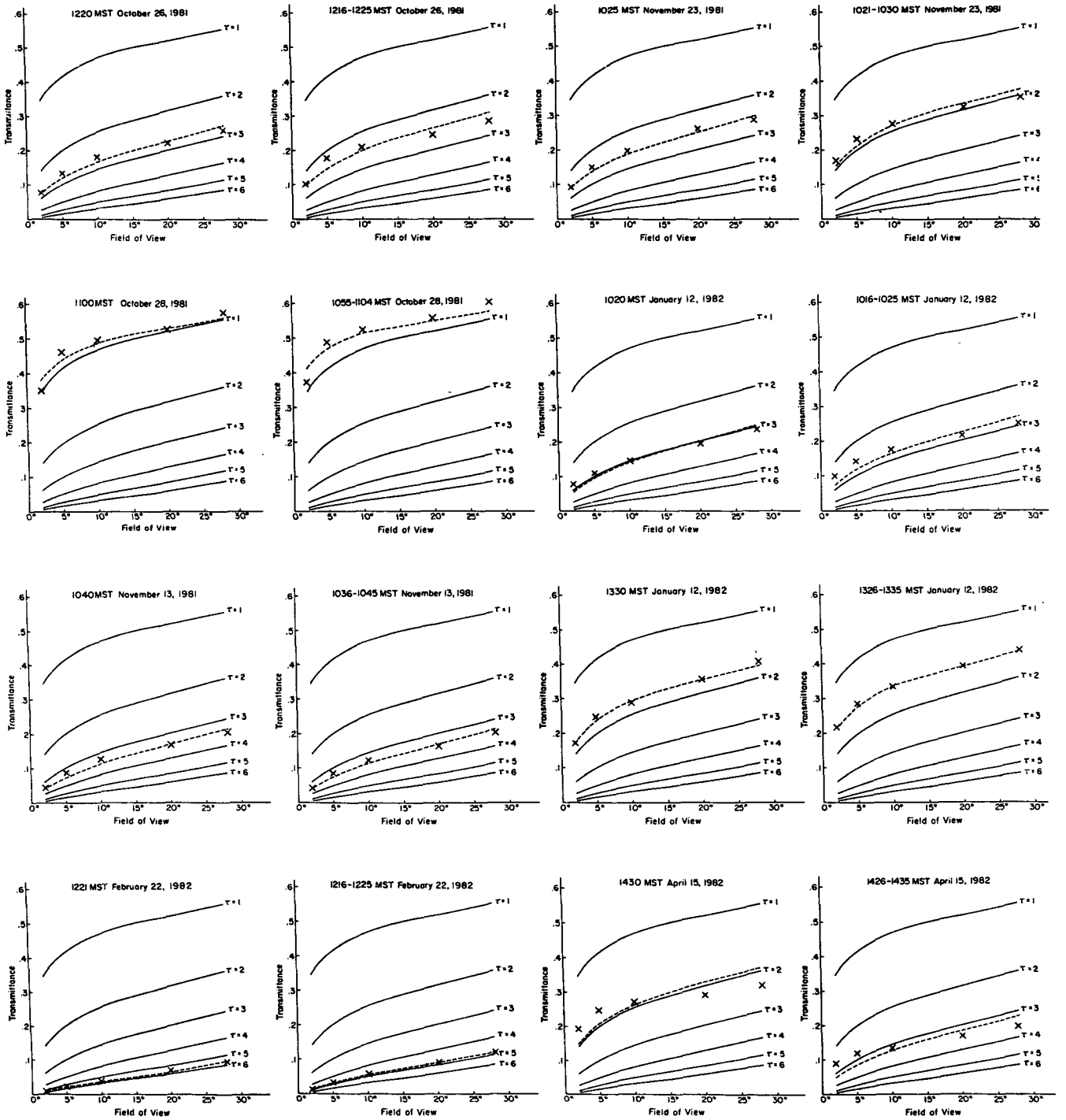

FIG. 3. Instantaneous and 10 min average field of view versus transmittance plots for various cloud scenes. Solid lines are model results; crosses are observed data points and the dashed line represents the best fit relationship.

present. The work of Jacobowitz (1971) indicates that for randomly oriented hexagonal ice crystals, intensity values are less for crystals than for spheres at scattering angles between 5° and 25°. This may explain some of the differences between model and experimental results.

To quantify the graphical predictions, optical depths were calculated using the methods described in Section 5a; a summary of the results of these calculations using 10 min average data is shown in Table 5. Columns A and B of the table list values of the optical depth calculated by using the method of the FOV average and

TABLE 5. Optical depth values derived from multiple field of view photodiode measurements.

Date	Time (LST)	Cloud type	Optical depth (A) FOV average	(B) ⟨rms⟩	(C) Maximum average	(D) Minimum FOV	(E) Maximum σ	(F) Minimum σ
28 Oct 1981	1100	High clouds Cirrus	0.85	0.86				
	1055–1104	Cirrostratus	0.75	0.77	0.98	0.58	0.118	0.064
26 Oct 1981	1220	High clouds	2.71	2.77				
	1216–1225	Cirrocumulus	2.43	2.44	3.45	1.58	0.262	0.116
13 Nov 1981	1040	High clouds	3.40	3.44				
	1036–1045	Cirrostratus	3.39	3.43	4.61	1.96	0.254	0.065
22 Feb 1982	1221	High clouds	5.58	5.57				
	1216–1225	Cirrostratus	4.93	4.96	5.65	4.61	0.284	0.072
23 Nov 1981	1025	Mid-level clouds	2.51	2.52				
	1021–1030	Altocumulus	1.91	1.91	3.57	0.57	0.280	0.037
12 Jan 1982	1020	Low clouds	3.00	3.05				
	1016–1025	Upslope stratus	2.70	2.74	3.56	2.06	0.347	0.074
12 Jan 1982	1330	Low clouds	1.75	1.76				
	1326–1335	Stratus	1.52	1.52	2.81	0.16	0.348	0.019
15 Apr 1982	1430	Low clouds	1.97	1.95				
	1426–1435	Cumulus	3.12	3.25	8.00	1.57	0.821	0.155

by finding the optical depth that produces the least rms error between model and experiment, respectively. The τ values producing the smallest rms errors between model and experiment (column B) correspond to the dashed curves in Fig. 3.

Columns C and D of Table 5 show the variability of the calculated optical depths over the various 10 min periods. As the values indicate, there was a significant range of values in all but the 28 October case. This would suggest that the cloud fields examined were not of uniform thickness, a situation which is not optimum for this inference but, nevertheless, quite realistic. The maximum range of calculated τ occurred on 15 April with values extending from 1.57 to 8.00. The broken cumulus field present at this time was obviously responsible for the large variation. The small range of τ on 28 October was observed in the presence of a thin cirrus cloud layer.

Although one might initially suspect that the technique described above applies only for horizontally homogeneous clouds, results presented by Welch *et al.* (1980) suggest otherwise. Welch *et al.* show that the average optical depth of a nonhomogeneous layer may be used to approximate the average bulk radiative properties of the layer; therefore one can interpret the results from the multi-FOV radiometer for the broken cloud case as an average optical depth over the field of view. Using this averaged or equivalent value of optical depth one is able to approximately reproduce the bulk radiative properties of the layer. Avaste and Vaynikko (1973) confirm this first order agreement; however, they go on to point out that the transmittance for the broken layer is invariably higher than that for the uniform, mean value of optical depth.

The five detectors were sampled at 1 min intervals, thus the 10 min average values consist of ten sets of five instantaneous samples. From each of these samples an optical depth can be deduced from Eq. (2) such that we have ten sets of five instantaneous estimates of the cloud optical depth. Columns E and F of Table 5 show the maximum and minimum standard deviations of optical depth among the ten instantaneous sample sets.

These values yield some indication of the horizontal variability of the cloud. Not unexpectedly, the 15 April case provides the largest value of 0.821. In fact, for all but the 28 October case, at least 1 min of each 10 min period examined showed a standard deviation that was greater than 0.25. By contrast, all but two of the 10 min periods produced a σ value that was less than 0.10. This supports the results in columns C and D which suggest the nonuniform nature of the cloud fields. This lack of uniformity was also confirmed by all sky photographs.

6. Conclusion

A method has been described which uses a photodiode radiometer to infer optical depth of thin clouds from solar radiance measurements. The photodiode radiometer measures incident radiation at angular fields of view of 2, 5, 10, 20 and 28°. These measurements were used to calculate values of transmittance for various cloud fields. The observations were compared with similar calculations derived from a Monte Carlo ra-

diative transfer model using a Best droplet distribution for horizontally infinite and homogeneous water clouds of optical depths 1 to 6 for the spectral bandpass of 0.3–2.8 μm.

Transmittance values derived from the model and from observations were compared for high, middle, and low cloud cases. A graphical comparison was made using plots of transmittance versus field of view for both model and experimental results. To verify the graphical prediction, an experimentally derived cloud optical depth was calculated for each field of view and the five values were then averaged. For each cloud case, instantaneous and 10 min average values were calculated.

Optical depths determined using both instantaneous and 10 min average values of transmittance were presented for eight cloud situations. The plots of transmittance versus field of view agreed very well with the model curves, especially for the instantaneous values of transmittance. The major exception was in the presence of a broken cumulus cloud field.

While one might initially suspect that the technique described above applies only for the horizontally homogeneous clouds, results presented by Welch *et al.* (1980) suggest otherwise. Welch *et al.* show that the average optical depth of a nonhomogeneous layer may be used to approximate the average bulk radiative properties of the layer; therefore one can interpret the results from the multi-FOV radiometer for the broken cloud case as an average optical depth over the field of view. Using this averaged or equivalent value of optical depth one is able to approximately reproduce the bulk radiative properties of the layer.

The results of the case studies showed a rather consistent pattern where the wider fields of view produced slightly larger optical depth estimates than the smaller fields of view. This may be due to nonhomogeneities in the cloud field causing less energy to reach the wide fields of view than would normally be the case. A second possible explanation is the fact that the Monte Carlo model results used a Best droplet distribution for spherical water drops while the case studies dealt mainly with ice clouds.

On the basis of the analysis of the case studies presented, the photodiode radiometer shows real promise as an effective tool for deducing optical depth of thin clouds. Results derived from the photodiode measurements showed exceptionally good agreement with theory for a variety of cloud types and cloud cover situations. The only exception occurred when a rather nonuniform cumulus cloud field was present.

The photodiode radiometer also shows potential for other uses. Since the 2° field of view instrument measures almost exclusively the direct solar beam, it could conceivably be used as a tool for determining sunshine duration. Other valuable information about the nature of the cloud cover could be gained by examining the standard deviation of the five field-of-view optical depths. In general, both clear sky and uniform cloud fields would produce small variability among the optical depths derived from the five photodiode radiometers while heterogeneous cloud fields would produce large variabilities.

Acknowledgments. The authors gratefully acknowledge the helpful dialogue and assistance provided throughout this work by Professor Thomas McKee and Dr. John Davis of the Department of Atmospheric Science at Colorado State University. This research was supported by the GARP project of the National Science Foundation under Grant ATM-8010691. Computer time was provided by the National Center for Atmospheric Research which is sponsored by the National Science Foundation.

REFERENCES

Avaste, O. A., and G. M. Vaynikko, 1973: The results of a calculation of the solar radiation fluxes reflected and transmitted by broken clouds. In Coll.: Statisticheskaya issledovaniya razorvannoy oblachnosti (Statistical studies of broken clouds). *Tr. MGK SSSR, Meteor.*, No. 21.

Best, A. C., 1951: Drop-size distribution in clouds and fog. *Quart. J. Roy. Meteor. Soc.*, **77,** 418–426.

Bowling, S. A., 1972: Comments on "Cirrus clouds and climate." *J. Atmos. Sci.*, **29,** 1003.

Cess, R. D., 1976: Climate change: An appraisal of atmospheric feedback mechanisms employing zonal climatology. *J. Atmos. Sci.*, **33,** 1831–1843.

——, and V. Ramanathan, 1978: Averaging of infrared cloud opacities for climate modeling. *J. of Atmos. Sci.*, **35,** 919–922.

Coulson, K. L., 1975: *Solar and Terrestrial Radiation.* Academic Press, 320 pp.

Cox, S. K., 1971: Cirrus clouds and climate. *J. Atmos. Sci.*, **28,** 1513–1515.

Davis, J. M., S. K. Cox and T. B. McKee, 1979: Total shortwave radiative characteristics of absorbing finite clouds. *J. Atmos. Sci.*, **36,** 508–518.

Ellis, J. S., 1978: Cloudiness, the planetary radiation budget and climate. Ph.D. dissertation, Colorado State University, 129 pp.

Jacobowitz, H., 1971: A method for computing the transfer of solar radiation through clouds of hexagonal ice crystals. *J. Quant. Spectrosc. Radiat. Transfer,* **11,** 691–695.

Manabe, S., and R. Strickler, 1964: Thermal equilibrium of the atmosphere with a convective adjustment. *J. Atmos. Sci.*, **21,** 361–385.

McKee, T. B., and S. K. Cox, 1974: Scattering of visible radiation by finite clouds. *J. Atmos. Sci.*, **31,** 1885–1892.

Noble, B., 1969: *Applied Linear Algebra.* Prentice Hall, 523 pp.

Ohring, G., and S. Adler, 1978: Some experiments with a zonally averaged climate model. *J. Atmos. Sci.*, **35,** 186–205.

——, and P. Clapp, 1980: The effect of changes in cloud amount on the net radiation at the top of the atmosphere. *J. Atmos. Sci.*, **37,** 447–454.

Stephens, B. L., 1978: Radiation profiles in extended water clouds. II: Parameterization schemes. *J. Atmos. Sci.*, **35,** 2123–2132.

Thompson, T. M., and S. K. Cox, 1982: Subtropical climatology of direct beam solar radiation. *J. Appl. Meteor.*, **21,** 334–338.

Twomey, S., 1976: Computations of the absorption of solar radiation by clouds. *J. Atmos. Sci.*, **33,** 1087–1091.

Welch, R. M., S. K. Cox and J. M. Davis, 1980: *Solar Radiation and Clouds. Meteor Monogr.*, No. 39, Amer. Meteor. Soc., 93 pp.